

Prague

6.11.–9.12.2006



# Diagnostic tool for lateral coupling

Report from RC LACE scientific stay

Scientific supervisor: Filip Váňa

Ján Mašek

SHMÚ, Jeséniova 17

833 15 Bratislava

Slovak Republic

E-mail: [jan.masek@shmu.sk](mailto:jan.masek@shmu.sk)

Typeset by L<sup>A</sup>T<sub>E</sub>X

# Contents

|          |  |           |
|----------|--|-----------|
| <b>1</b> | <b>Introduction</b>  | <b>3</b>  |
| <b>2</b> | <b>Design of diagnostic tool</b>                                       | <b>4</b>  |
| 2.1      | LAM domains . . . . .  | 4         |
| 2.2      | Integration period . . . . .   | 5         |
| 2.3      | Common integration settings . . . . .                                  | 6         |
| 2.4      | LBC filtering . . . . .  | 6         |
| 2.5      | Choice of parameter, level and scores . . . . .                        | 7         |
| 2.6      | Qualitative comparison of vorticity fields . . . . .                   | 9         |
| <b>3</b> | <b>Basic tests of Davies relaxation scheme</b>                         | <b>11</b> |
| 3.1      | Sensitivity to initial state . . . . .                                 | 12        |
| 3.2      | “No relaxation” test . . . . .   | 12        |
| 3.3      | Sensitivity to coupling frequency . . . . .                            | 14        |
| 3.4      | Comparison of linear and quadratic couplings . . . . .                 | 16        |
| 3.5      | Impact of biperiodicization and “problem” of ultralong waves . . . . . | 17        |
| 3.6      | Spectral composition of RMSE . . . . .                                 | 17        |
| <b>4</b> | <b>Conclusions</b>   | <b>19</b> |
| <b>A</b> | <b>Where to find what</b>  | <b>21</b> |
| <b>B</b> | <b>Brief description of developed FA utilities</b>                     | <b>22</b> |
| <b>C</b> | <b>Important remark on vorticity postprocessing</b>                    | <b>22</b> |

# 1 Introduction

Lateral boundary treatment is a critical issue for limited area models (LAM). Success of these models is based on the fact that for lower atmospheric levels small scale phenomena are driven primarily by interaction with surface. Approximate knowledge of large scale flow provided by driving model is then sufficient for realistic simulation of these finer scale features in nested LAM. In simplest case (one way nesting) there is no information transferred from nested model back to driving model. Such approach is justified if the mean effect of small scales is properly parameterized in driving model or if the interaction of small scales towards larger ones is weak (i.e. their parameterization in driving model is not needed). Without parameterization of relevant physical phenomena driving model would not be able to provide reliable large scale flow. (For example, ignoring of gravity wave drag due to subgrid orography has disastrous effect on model performance if the horizontal resolution is not high enough.)

One way nesting has big advantage for operational numerical weather prediction (NWP) – driving model is independent from its nested models and can be computed in distant location. Limited capacity of telecommunication lines makes two way nesting impossible in such conditions. However, there are two problems inherent to one way nesting. First problem is fundamental, second one is more technical:

1. Mathematical formulation of lateral boundary treatment.

This problem is complicated since lateral boundaries are opened and they should behave transparently. It means that they should transfer signals entering LAM domain from driving model to nested model. At the same time they should absorb signals leaving LAM domain. Ideally, initial-boundary value problem should be well posed, but in NWP practice it usually have to be overdetermined with some ad hoc treatment to reduce noise generated by misfit between driving and nested solutions. Moreover, as was pointed out by Durran [2], even perfectly transparent boundaries have some limitations coming from one way nesting strategy.

2. Insufficient frequency of lateral boundary conditions (LBC) provided by driving model.

Driving model is usually integrated with longer timestep than nested model, therefore it provides LBC with lower frequency than needed. Even more restrictive factor for LBC frequency is capacity of telecommunication lines when driving model is operated at distant location. For timesteps where LBC are missing, nested model must estimate them by interpolation in time. As a result, some frequencies which were correctly resolved in driving model will be undersampled and aliased in nested model. This is typically problem for small, rapidly moving weather systems entering the LAM domain.

Moving towards higher resolutions and more sophisticated NWP models with complex physical packages necessarily brings significant increase of computational costs. When available computer power does not increase with the same speed, one is forced to reduce size of operational LAM domains. For small domains, however, solution becomes dominated by LBC after very short time. This fact puts coupling issue into centre of interest and calls for its reexamination.

If alternatives are to be tested, one must be able to analyze errors coming from coupling scheme. Main objective of this stay was therefore to propose, implement and test diagnostic tool for evaluating performance of coupling scheme in full 3D ALADIN. Design of such tool rises several questions:

- How long integration is needed?
- Which fields and levels to look at?
- Is subjective verification sufficient?
- If not, which scores to evaluate?

Once ready, tool was used to evaluate performance of current Davies relaxation scheme and to reveal some of its limitations.

## 2 Design of diagnostic tool

Delivered diagnostic tool is far from compact piece of software. It is rather set of recipes, recommendations, few scripts and utilities. Its design was strongly influenced by comprehensive work of Elía et al. [3]. In this paper authors introduce so called *perfect model approach* which enables to isolate errors caused by coupling scheme from other sources of model error. This is exactly what was needed in order to evaluate performance of coupling scheme. Moreover, paper contains many valuable recommendations about how to carry out numerical experiments and interpret the results.

Perfect model approach is based on very simple idea. It computes the same LAM on two domains, large and small, with identical resolution and matching gridpoints. Integration on large domain is used as perfect reference, it can be coupled e.g. to global model. Integration on small domain represents nested LAM, with LBC taken from perfect reference. In order to simulate jump in resolution between driving and nested models, short scales are filtered out from LBC.

### 2.1 LAM domains

Large domain for computing perfect reference (denoted MFST) was taken from MFSTEP project. More specifically, it was old MFSTEP domain covering central and southern Europe, eastern Atlantic, Mediterranean Sea, Black Sea and north of Africa (figure 1). For this domain LBC from ARPEGE interpolated to target resolution  $\Delta x = \Delta y = 9.5$  km were available with 3 hour frequency.

Small domain for testing coupling scheme (denoted DOM1) was chosen as square, with side approximately 50 % of north–south dimension of domain MFST. Its centre was shifted 15 gridlengths to the east and 12 gridlengths to the north from centre of domain MFST<sup>1</sup>, so that it contains Alps and boundary intersections with main mountain ranges are minimized. Southern half of boundary lies above Mediterranean sea, the rest lies above land (figure 2). Horizontal resolution was the same as for domain MFST.

Details about both domains are listed in table 1. Standard ALADIN notations are used: ‘C’ is central zone surrounded by intermediate zone ‘I’ where Davies relaxation is applied and ‘E’ is artificial extension zone needed for biperiodicization of fields. Spectral truncation for both domains was linear, only orography was quadratically truncated. It means that shortest represented wave was  $3\Delta x$  for orography and  $2\Delta x$  for other fields. All experiments used 37 vertical levels.

---

<sup>1</sup>More precisely, shifts were done along  $x$  and  $y$  axes.

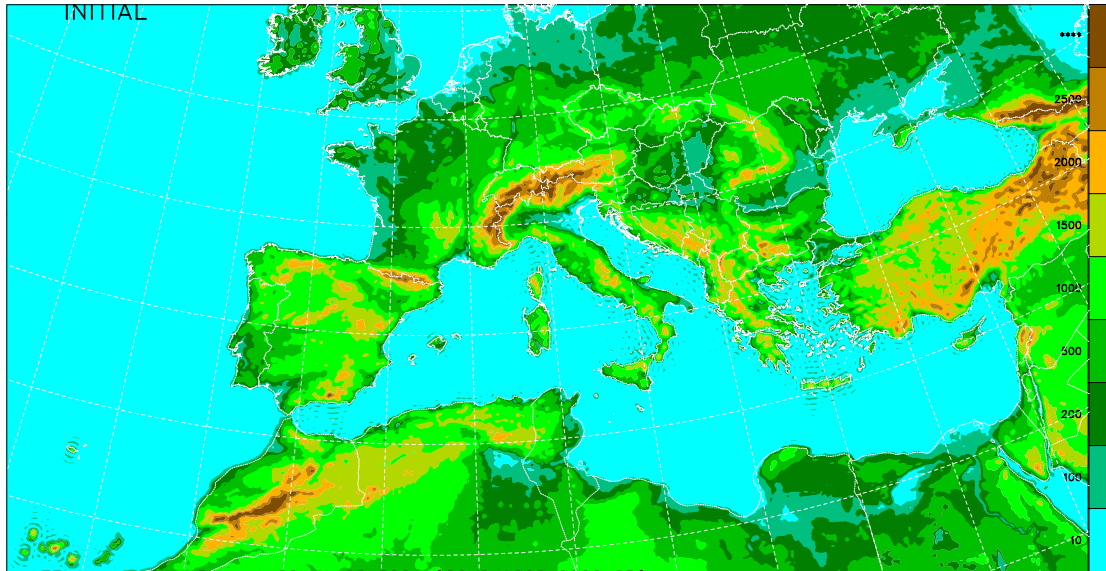


Figure 1: Domain MFST and orography of driving model used as perfect reference.

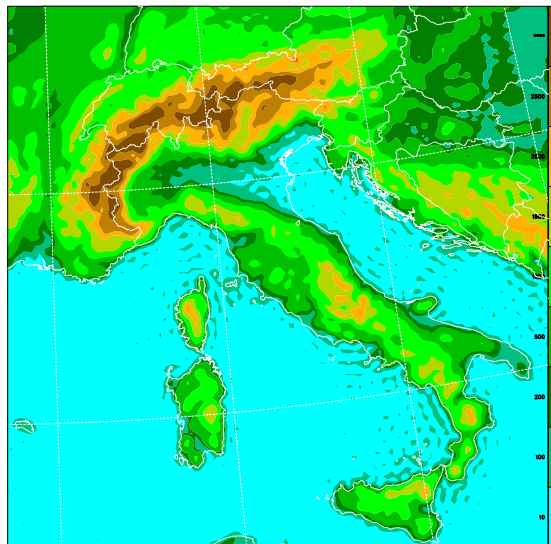


Figure 2: Domain DOM1 and orography of nested model used for coupling experiments.

| domain | size C + I       | size C + I + E   | truncation       |
|--------|------------------|------------------|------------------|
| MFST   | $589 \times 309$ | $600 \times 320$ | $299 \times 159$ |
| DOM1   | $139 \times 139$ | $150 \times 150$ | $74 \times 74$   |

Table 1: Size and truncation of driving and nested domains. Horizontal resolution was  $\Delta x = \Delta y = 9.5$  km, default width of I zone 8 points.

## 2.2 Integration period

First decade of April 2005 was selected as testing period. It can be characterized by typical unstable spring weather with prevailing zonal circulation and alternating cyclonic and anticyclonic situations.

Reference 10 day integration on MFST domain started on 01-Apr-2005, 00 UTC. It was run as reanalysis, i.e. coupled with ARPEGE analyses and 3 hour forecasts (available

4 times per day). Like this, coupling frequency for reference integration was 3 hours.

Nested integrations on domain DOM1 started also on 01-Apr-2005, 00 UTC. Integration length was 10 days for experiments with 3 hour coupling frequency, 2 days for 1 hour coupling frequency and 12 hours for experiments with LBC file available at every timestep.

### 2.3 Common integration settings

Presented experiments were done with hydrostatic version of model ALADIN, cycle al29t2mxl. Model settings except from geometry and timestep were identical to ALADIN/CE operational suite (Prague, Nov-2006). Main highlights are two time level semi-implicit scheme with semi-Lagrangian advection, timestep  $\Delta t = 400$  s and semi-Lagrangian horizontal diffusion. If not stated otherwise, coupling frequency was 3 hours and LBC were interpolated quadratically in time (LQCPL = .T.). Width of relaxation zone was 8 points by default.

### 2.4 LBC filtering

In practice, horizontal resolution of driving model is lower than that of nested model. In ALADIN community cascade of coupled models is usually chosen in such way that jump in resolution between driving and nested models does not exceed factor 3.<sup>2</sup> Therefore, it was decided to carry out coupling experiments with jump in resolution equal to 3, which should be the least favourable value occurring in ARPEGE/ALADIN world.

Resolution jump was simulated by removing the short scales from LBC. Procedure consisted of two steps:

1. Configuration EE927 without use of climate files (MFST  $\rightarrow$  DOM1).

Thanks to matching gridpoints configuration EE927 did not perform horizontal interpolations. It only extracted fields for C + I part of domain DOM1, biperiodicized them and performed spectral fit.<sup>3</sup>

2. Spectral filtering of 3D prognostic fields (horizontal wind, temperature and specific humidity) along eta levels.

Surface geopotential (orography) was not filtered since it is always available in full resolution for nested run. Surface pressure representing total column mass was not touched either, in order to keep its consistency with orography. Anyway, filtered state was imbalanced due to smoothing of 3D prognostic fields performed along eta levels. This is not a problem since in realistic NWP conditions there is always some LBC imbalance introduced by interpolations.

First step gave LBC for domain DOM1 in full resolution, second step removed small scale information from 3D prognostic fields. Instead of sharp cut-off, soft spectral filter

---

<sup>2</sup>Experience of other NWP consortia suggest that Davies relaxation scheme can safely withstand even higher jumps in resolution – at least up to 6 or 8.

<sup>3</sup>Due to bug in configuration EE927 some surface fields were not initialized correctly in extension zone when horizontal interpolations were skipped. This bug was assumed to be safe since it influenced only surface gridpoint fields and only in artificial extension zone. However, it prevented usage of climate files when configuration EE927 was run on matching grids. According to Ryad El Khatib bug is not present in pre-cycle 32.

was used in order to suppress generation of Gibbs waves. It had the form:

$$c_{m,n}^{\text{flt}} = c_{m,n} \cdot f(r_{m,n})$$

$$f(r) = \begin{cases} 1 & ; \quad r \leq r_1^{\text{crit}} \\ \frac{1}{2} + \frac{1}{2} \cos \left[ \pi \frac{r - r_1^{\text{crit}}}{r_2^{\text{crit}} - r_1^{\text{crit}}} \right] & ; \quad r_1^{\text{crit}} < r \leq r_2^{\text{crit}} \\ 0 & ; \quad r > r_2^{\text{crit}} \end{cases} \quad (1)$$

$$r_{m,n} = \sqrt{\left(\frac{m}{M}\right)^2 + \left(\frac{n}{N}\right)^2}$$

Symbols  $c_{m,n}^{\text{flt}}$  and  $c_{m,n}$  denote filtered and unfiltered spectral coefficients corresponding to wavenumbers  $m, n$ ;  $f(r)$  is filtering function;  $M, N$  are truncations in directions  $x, y$  and  $r_{m,n}$  is relative wavenumber determining position inside spectral ellipse (0 at centre, 1 at perimeter).

In order to simulate jump in resolution 3, filter parameters had values  $r_1^{\text{crit}} = 0$  and  $r_2^{\text{crit}} = \frac{1}{3}$ . It means that for linear truncation filter removed all waves shorter than  $6\Delta x$ , it did not touch mean value and it partially damped waves in between. Setting  $r_1^{\text{crit}} = r_2^{\text{crit}} = \frac{1}{3}$  would sharply cut-off all waves shorter than  $6\Delta x$ .

## 2.5 Choice of parameter, level and scores

To evaluate downscaling ability of LAM, Elía et al. [3] analyzed vorticity field at 850 hPa level. Their choice was based on the fact that vorticity spectra has considerable energy in the small scales, which simplifies identification of small perturbations. Level 850 hPa is high enough not to be disrupted by orography, but low enough to display substantial energy in the small scales. As for scores, authors concentrated on standard deviation and root mean square error (RMSE), both normalized by standard deviation of reference run. Important step was scale analysis of the scores.

Selection of parameter and scores made in [3] was adopted also for this work. However, choice of 850 hPa level was revisited. There were two reasons for this. First, horizontal mesh size used in [3] was almost 5 times higher ( $\Delta x = 45$  km), leading to less steep orography. Second, influence of orography to vorticity spectrum at given pressure level surely depends on choice of geographical domain.

In order to avoid confusion, it is necessary to define what is meant by vorticity. Throughout this work vorticity will refer to quantity:

$$\xi = m^2 \left[ \frac{\partial}{\partial x} \left( \frac{v}{m^2} \right)_p - \frac{\partial}{\partial y} \left( \frac{u}{m^2} \right)_p \right] \quad (2)$$

$$m = m(x, y) \quad u = \dot{x} \quad v = \dot{y}$$

Symbol  $m$  denotes map factor;  $x, y$  are conformal map coordinates and  $u, v$  are corresponding components of wind velocity. It should be stressed that horizontal derivatives in expression (2) are computed *along pressure levels*.<sup>4</sup> Vorticity (2) on pressure levels can be postprocessed directly by fullpos, but it is necessary to keep correct order of vertical interpolations and computation of horizontal derivatives. See appendix C for more details.

Plot 3a shows reference spectral profiles of vorticity variance for 5 different pressure levels, computed over nested domain DOM1 without 8 point boundary zone and averaged

<sup>4</sup>Thanks to small slope of pressure levels, quantity (2) is very close to vertical component of 3D relative vorticity  $\xi = \nabla \times \mathbf{v}$  (where  $\mathbf{v}$  denotes 3D wind velocity relative to the Earth).

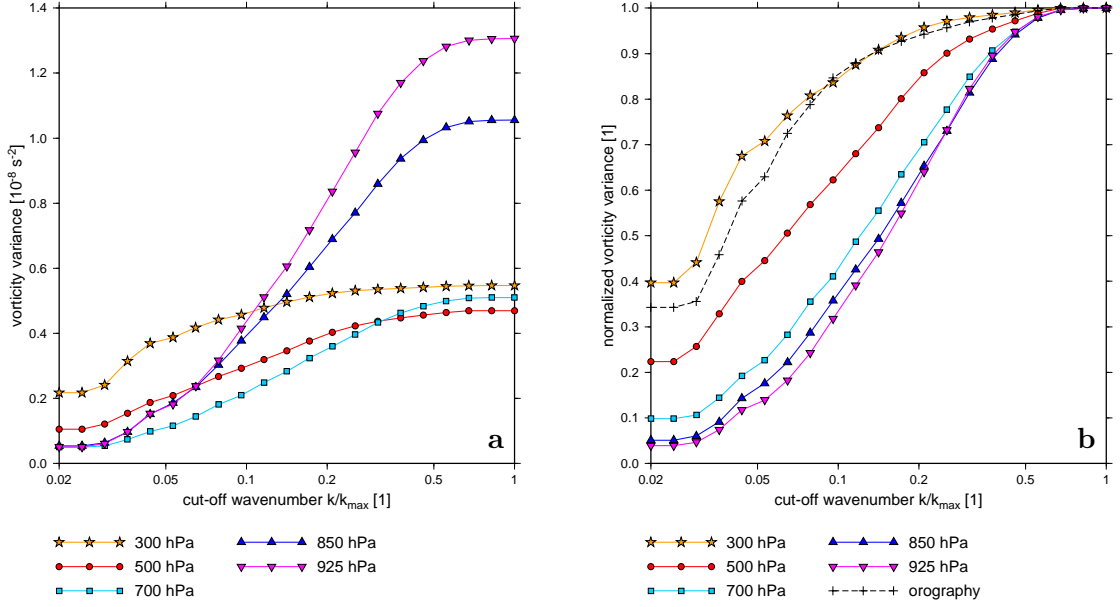


Figure 3: Dependency of spatial vorticity variance (a) and its normalized value (b) on relative cut-off wavenumber. Reference integration, variances computed over nested domain DOM1 without 8 point boundary zone and averaged over 10 day integration period.

over 10 day integration window (with step 12 hours). On horizontal axis is relative cut-off wavenumber  $r = k/k_{\max}$ . For given  $r$ , all wavenumbers greater than  $rk_{\max}$  (i.e. all wavelengths shorter than  $\lambda_{\min}/r$ ) were filtered out from vorticity field before computing the scores. Value  $r = 1$  means unfiltered field, value  $r = 0.5$  means removed wavelengths shorter than  $4\Delta x$ , and so on.

It can be seen that unfiltered vorticity variance ( $r = 1$ ) is highest at 925 hPa level and decreases as one moves upwards. It is lowest at 500 hPa level, then it slightly increases. Values for 300, 500 and 700 hPa levels are rather close. Profiles on the right part of the plot are almost horizontal, indicating that wavelengths between  $2\Delta x$  and  $3\Delta x$  practically do not contribute to vorticity variance. Large scale vorticity variance (left part of the plot) is highest at 300 hPa level and it decreases as one moves downwards. It is almost identical for levels 700, 850 and 925 hPa. For all levels largest contribution to vorticity variance comes from intermediate scales where the slope is steepest.

Plot 3b shows spectral profiles of vorticity variance normalized by its unfiltered value. In other words, it displays relative contribution of various scales to total vorticity variance. It can be observed that relative contribution of large scales is highest at 300 hPa level and decreases monotonically when going downwards. For comparison, spectral profile of normalized orography variance is also shown (black dashed line). There is no contribution from wavelengths between  $2\Delta x$  and  $3\Delta x$  since orography was quadratically truncated.

Evolution of vorticity standard deviation during 10 day reference integration is shown on plot 4a. It can be seen again that 925 and 850 hPa levels have highest variability. Moreover, spatial variability at these levels strongly depends on synoptic situation, reaching minimum in the middle of integration period. Spatial variability at remaining levels is somewhat weaker, on average it is lowest for 500 hPa level.

In order to find level most sensitive to lateral boundary treatment, 10 day nested integration with perfect initial state and filtered LBC was performed. For each level

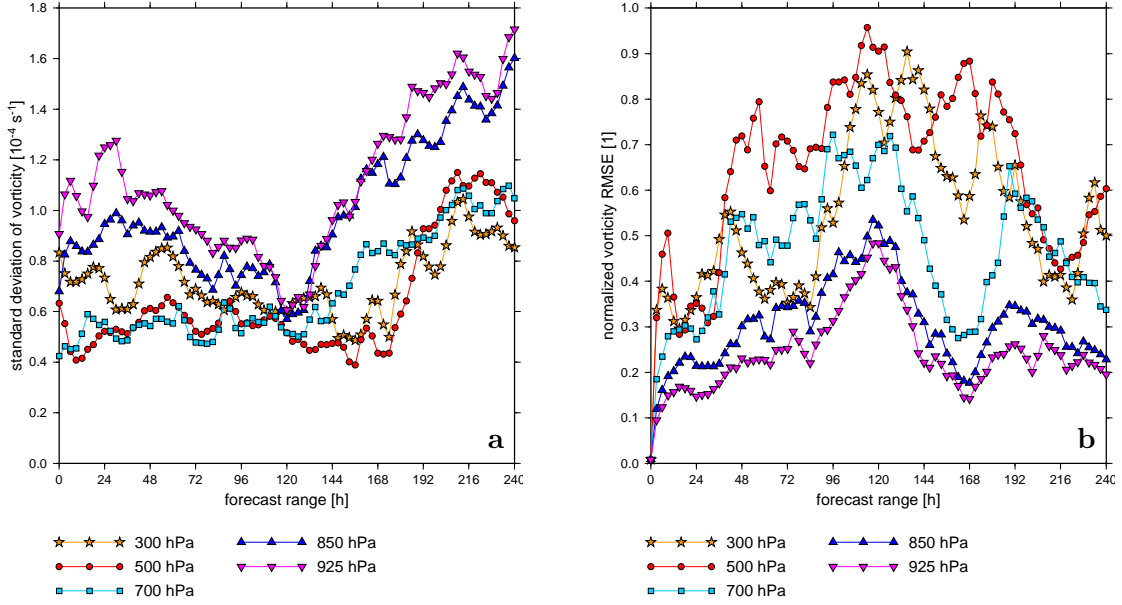


Figure 4: Evolution of vorticity standard deviation for 10 day reference integration (a) and normalized RMSE difference for nested run with perfect initial state and filtered LBC. Scores computed over nested domain DOM1 without 8 point boundary zone.

forecast skill was measured by RMSE difference from reference solution, normalized by standard deviation of reference field. Scores were again computed over nested domain DOM1 without 8 point boundary zone (i.e. omitting relaxation zone). Advantage of normalized RMSE is that it enables to compare forecast skill for fields with different variances. If reference field was estimated by its mean value, normalized RMSE would be 1. When forecasted and reference fields have the same mean value and variance but are uncorrelated, normalized RMSE is  $\sqrt{2}$ . This value can be interpreted as no skill at all.

Evolution of normalized vorticity RMSE during 10 day nested integration is shown on plot 4b. It can be seen that after period of fast initial growth (approximately first 48 hours) error saturates and then fluctuates around asymptotic value. Highest skill with normalized RMSE around 0.3 is displayed by vorticity at 925 and 850 hPa levels. This is not surprising since for unresolved convection low level wind field is built mostly as orographic response to large scale flow. It is then natural that orographically induced small scale features are easier to predict. Lowest skill is displayed by vorticity at 500 hPa level with normalized RMSE fluctuating around 0.7, occasionally approaching value 1. Therefore, it was decided to use 500 hPa level for evaluation of vorticity scores. This level gives the strictest measure of forecast skill.

## 2.6 Qualitative comparison of vorticity fields

Main weakness of introduced objective scores is that they do not contain information about spatial error structure. It is therefore useful to have a look at maps of vorticity and its error. Such subjective evaluation can give answer to questions whether error is localized mostly close to lateral boundaries or rather uniformly distributed throughout the domain, whether it is dominated by similar scales as vorticity field itself, and so on.

Figures 5 and 6 compare vorticity field at 500 hPa level computed by reference run against the same field computed by nested run on domain DOM1 with perfect initial

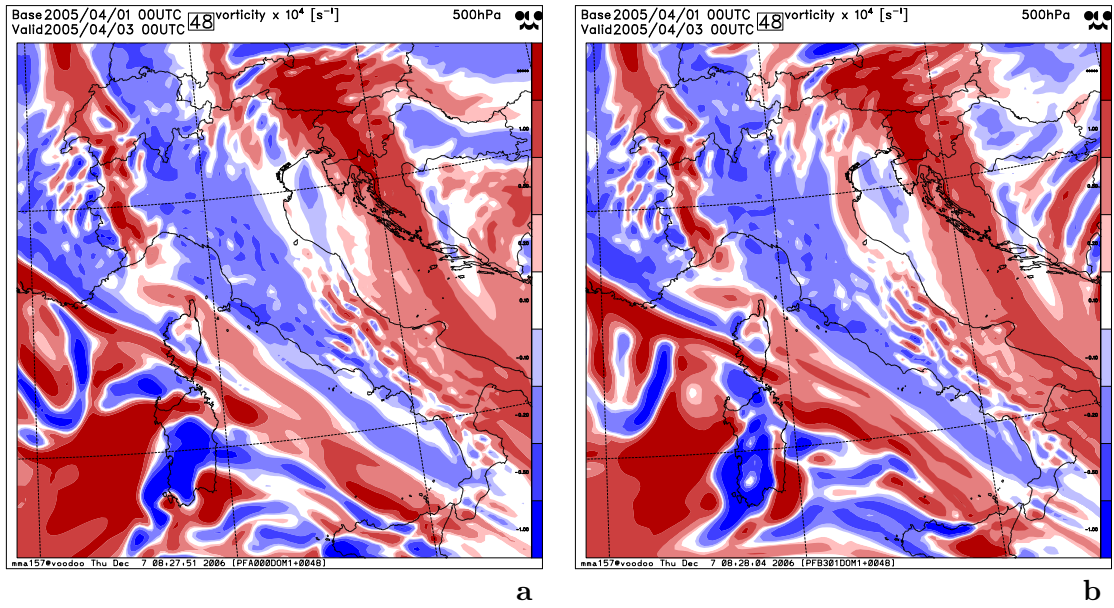


Figure 5: Vorticity at 500 hPa level for reference run (a) and nested run with perfect initial state and filtered LBC (b). State at  $t = +48$  h. I zone is omitted.

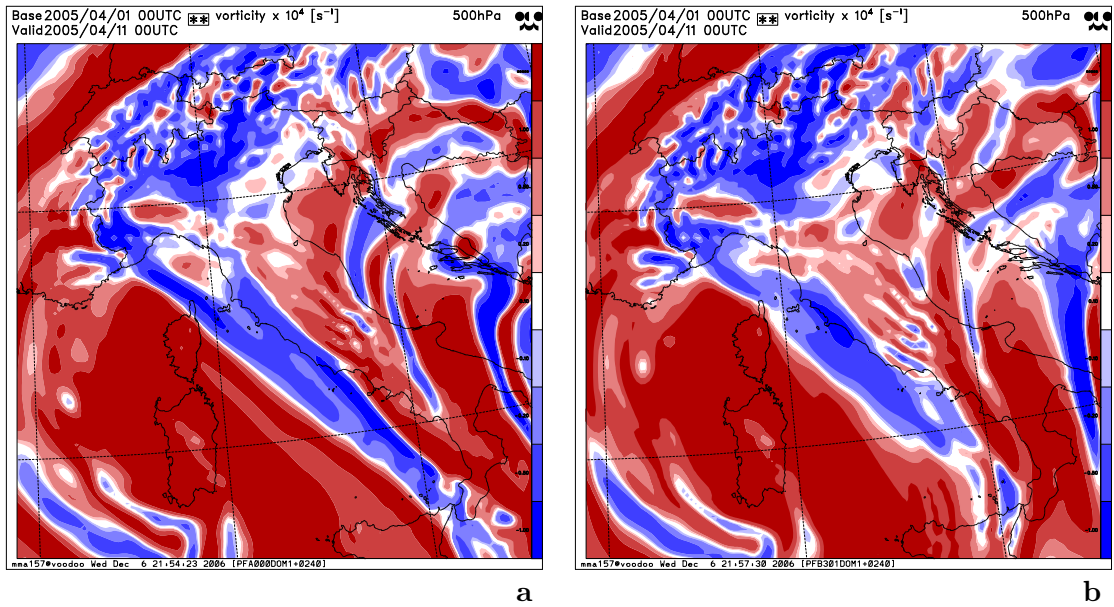


Figure 6: Vorticity at 500 hPa level for reference run (a) and nested run with perfect initial state and filtered LBC (b). State at  $t = +240$  h.

state and filtered LBC. It can be concluded that for both 2 day forecast (figure 5) and 10 day forecast (figure 6) large scale features are in good qualitative agreement. More careful inspection shows, however, that some smaller scale details are significantly different.

Vorticity error at 500 hPa level (i.e. difference of plots 5b – 5a, resp. 6b – 6a) is plotted on figure 7, using the same contouring levels. After 2 days error reaches magnitude of reference vorticity field in substantial part of domain (plot 7a), after 10 days practically in all domain (plot 7b). Large scales present in reference vorticity field cannot be seen in error field which is dominated by intermediate scales.

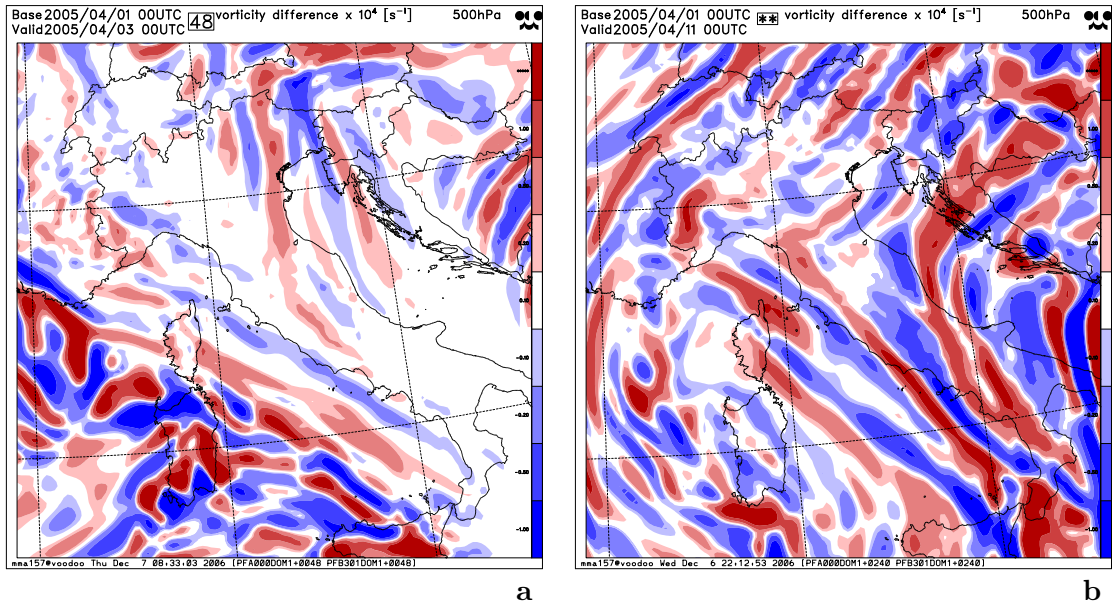


Figure 7: Vorticity error at 500 hPa level for nested run with perfect initial state and filtered LBC. State at  $t = +48$  h (a) and  $t = +240$  h (b). Contouring levels are the same as on figures 5 and 6.

Main features of proposed diagnostic tool can be summarized now. It is based on perfect model approach [3], using the same LAM on two domains, large and small, with identical resolution and matching gridpoints. Reference solution is obtained by 10 day LAM integration on large domain coupled with analyses. Jump in resolution between driving and nested LAM is simulated by LBC filtering based on cosine spectral filter (1). Performance of coupling scheme is judged from vorticity field (2) at 500 hPa level. It is not so strongly orographically driven as levels below, but it still contains sufficient proportion of finer scale details. Subjective evaluation can be done visually by comparing vorticity maps, resp. by inspection of vorticity departure from reference solution. More objective measure is provided by scores computed over target domain. Normalized standard deviation indicates whether nested integration realistically reproduces variability of vorticity field. Normalized RMSE difference from reference solution is a strict measure of forecast skill. Its asymptotic value estimated from 10 day nested integration seems to be a suitable indicator for comparing performance of various coupling schemes. Further insight can be gained by examining spectral composition of scores.

### 3 Basic tests of Davies relaxation scheme

Having diagnostic tool ready, its usage can be demonstrated on Davies relaxation scheme implemented in model ALADIN. Objective is to analyze basic behaviour of the coupling scheme and its sensitivity to various factors like quality of initial state, LBC filtering, coupling frequency, type of LBC interpolations in time, biperiodicization, etc.

### 3.1 Sensitivity to initial state

It is well known fact that in LAM integration influence of initial state diminishes with time and the solution becomes dominated by LBC. For this reason positive impact of LAM data assimilation can be seen only in early stages of the forecast. This effect can be easily simulated with perfect model approach.

Plot 8a shows results of perfect twin experiment representing upper limit for performance of Davies relaxation scheme with 3 hour coupling frequency. In this experiment nested integration used unfiltered both initial state and LBC. It can be seen that while normalized standard deviation fluctuates only slightly around perfect value 1, normalized RMSE grows during first 48 hours and then saturates around value 0.7. Perfect twin is not perfect, which can be attributed mainly to insufficient coupling frequency. Two other sources of error responsible for departure from reference solution are biperiodicization of fields and approximate implementation of Davies relaxation scheme inside semi-implicit timestepping.

Plots 8b–8d show evolution of scores in realistic NWP conditions with filtered LBC and different initial states. When initial state is filtered but uninitialized, strong spinup occurs during first 24 hours (plot 8b). Digital filter initialization deteriorates scores for analysis, but it substantially reduces subsequent spinup (plot 8c). Early forecast can be further improved by using perfect initial state (plot 8d). This experiment represents upper limit for improvement which can be expected from LAM data assimilation.

Plot 8e shows results of very tough test with flat initial state. Initial 3D prognostic fields were made constant along eta levels by filtering out all wavenumbers greater than zero (in other words, field on given eta level was reset to its mean value along that level). After period of excessively strong spinup realistically looking solution developed from filtered LBC. This is illustrated on figure 9 which compares vorticity field after 48 hours with that of perfect twin experiment. Differences between these two extreme cases are no more significant than differences between plots 5a and 5b. Comparison of plots 9b and 5b further illustrates that influence of initial state after 2 day integration is very weak.

It is worth mentioning that scores on plots 8b–8e are almost identical for days 3–10 and not much worse than scores for perfect twin experiment (plot 8a). From this point of view costly increase of LBC resolution does not bring much benefit, while improvement of initial state can dramatically increase quality of early forecast. This result is in full agreement with [3] and it should be strong argument in favour of LAM data assimilation.

### 3.2 “No relaxation” test

In order to see benefit brought by Davies relaxation scheme, experiment with perfect initial state and filtered LBC (plot 8d) was repeated with zero relaxation zone (plot 8f). In this configuration all prognostic variables were prescribed on lateral boundaries, but there was no sponge zone which would absorb noise coming from overdetermination. In such conditions one should get strongly deteriorated forecast, which was really the case. Fluctuations of normalized standard deviation around perfect value 1 are much stronger than for experiment with 8 point relaxation zone. Normalized RMSE saturates around value 1.2, occasionally reaching value  $\sqrt{2}$ . Forecast with such scores has very limited skill.

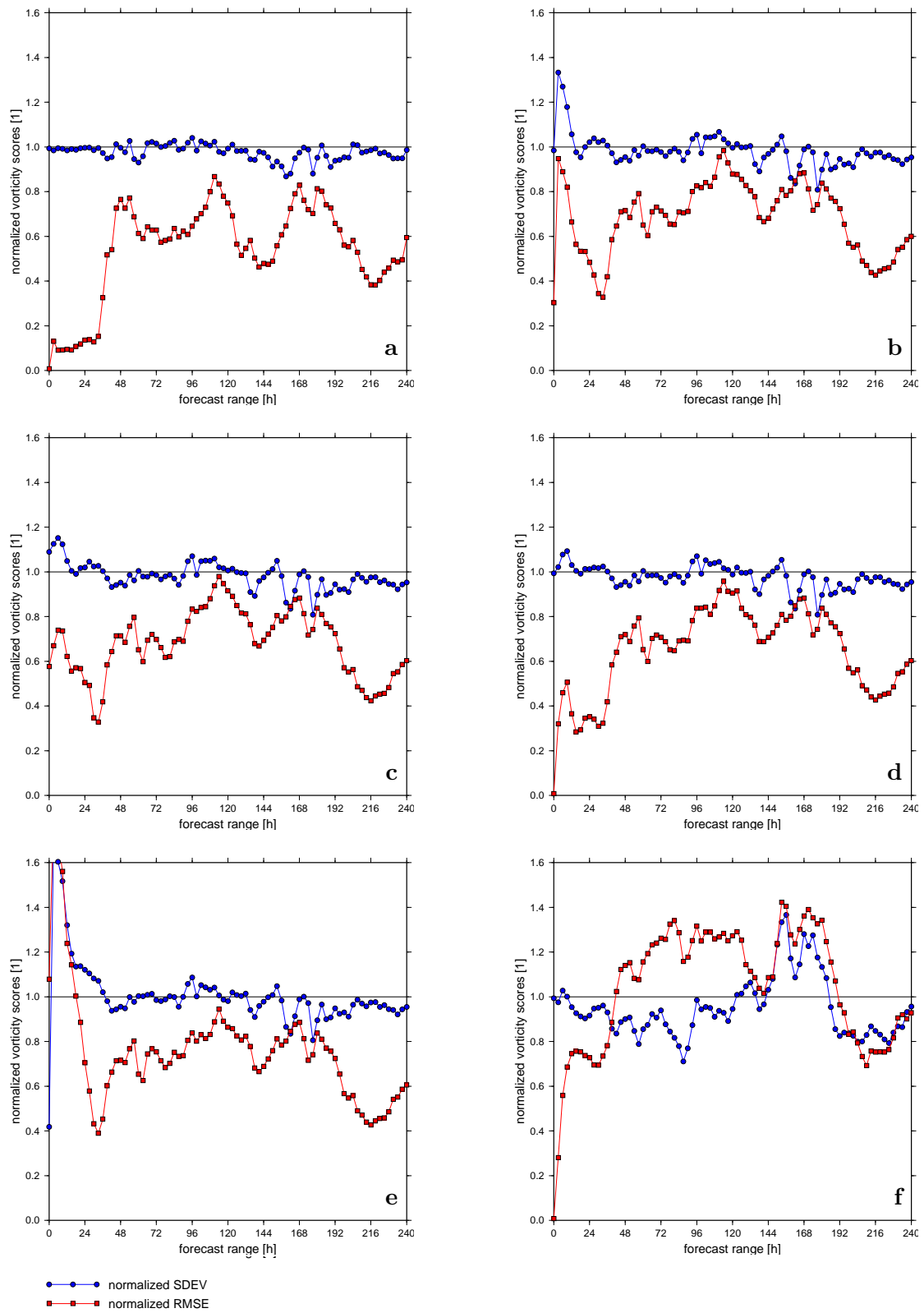


Figure 8: Evolution of normalized vorticity scores at 500 hPa level computed over nested domain DOM1 without 8 point boundary zone. Experiment (a) used perfect initial and lateral boundary conditions, experiments (b)–(f) used filtered LBC with different initial states: filtered (b), filtered and initialized (c), perfect (d), flat (e), perfect again but coupling done without relaxation zone (f).

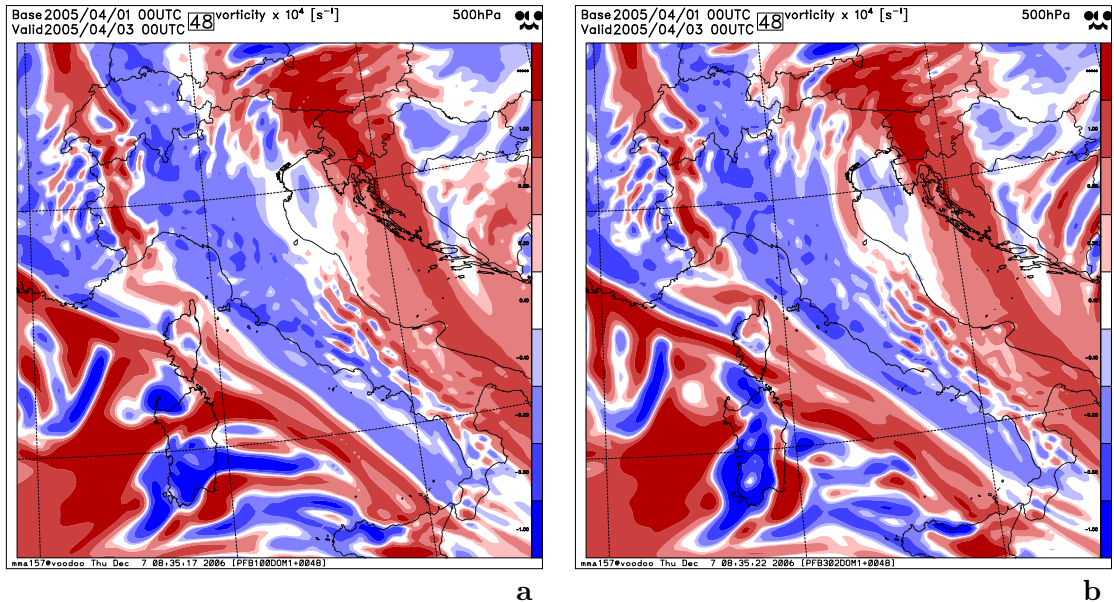


Figure 9: Vorticity at 500 hPa level for nested runs with perfect initial state and perfect LBC (a) and with flat initial state and filtered LBC (b). State at  $t = +48$  h, to be compared with figure 5.

### 3.3 Sensitivity to coupling frequency

As was seen earlier, perfect twin experiment with 3 hour coupling frequency does not reproduce reference solution. In order to examine influence of coupling frequency, experiment was repeated with LBC provided every hour and every timestep. Integration was shortened to 12 hours because the volume of coupling files produced at every timestep was huge.

Evolution of normalized vorticity RMSE for coupling frequencies 3 h, 1 h and 400 s ( $27\Delta t$ ,  $9\Delta t$  and  $\Delta t$ ) is shown on figure 10 (range of vertical axis is smaller than on figure 8). First it should be noticed that scores do not start from zero even if initial state was perfect. This can be probably attributed to biperiodicization and spectral fitting of fields performed in configuration EE927 when going from driving domain MFST to nested domain DOM1.<sup>5</sup> During first few hours scores for all three experiments are almost identical. After 6 hours, at the end of weak spinup period, normalized RMSE for 3 hour coupling frequency is already separated from the other two curves. Until the end of integration window it keeps roughly twice bigger value than normalized RMSE for 1 hour coupling frequency. Surprisingly, increase of coupling frequency from 1 hour to every timestep hardly brings any additional improvement. Therefore, going beyond 1 hour coupling frequency seems to be useless.

As the next step sensitivity to coupling frequency in more realistic conditions with perfect initial state and filtered LBC was studied. Original experiment with 3 hour coupling frequency was rerun with 1 hour coupling frequency. This time integration window was shortened to 48 hours.

Evolution of normalized vorticity RMSE for coupling frequencies 3 h and 1 h is shown on figure 11 (range of vertical axis differs from figures 8 and 10). Imperfect LBC cause approximately 4 times stronger spinup than for perfect twin experiment. Spinup period is longer, it now takes about 15 hours. Solution with 1 hour coupling frequency starts

<sup>5</sup>Because of elliptical truncation there are less degrees of freedom in spectral space than in gridpoint space even if linear grid is used.

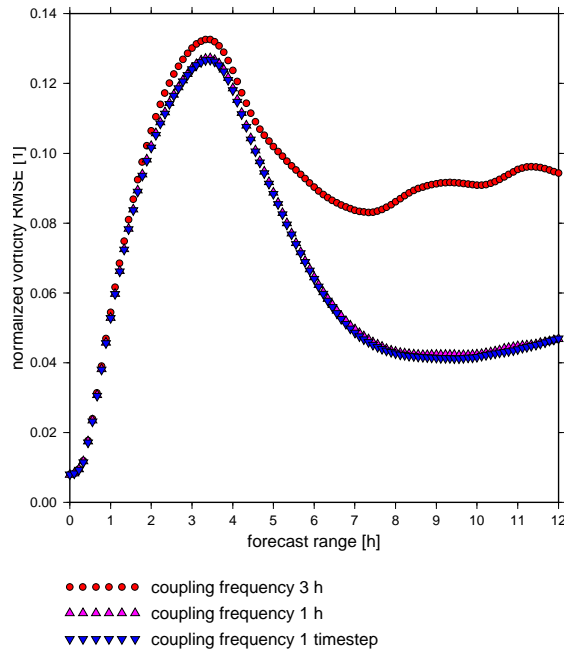


Figure 10: Sensitivity to coupling frequency for perfect LBC. Evolution of normalized vorticity RMSE at 500 hPa level computed over nested domain DOM1 without 8 point boundary zone. Nested runs with perfect initial state and coupling frequencies  $27\Delta t$ ,  $9\Delta t$  and  $\Delta t$ . Both driving and nested model timesteps were  $\Delta t = 400$  s.

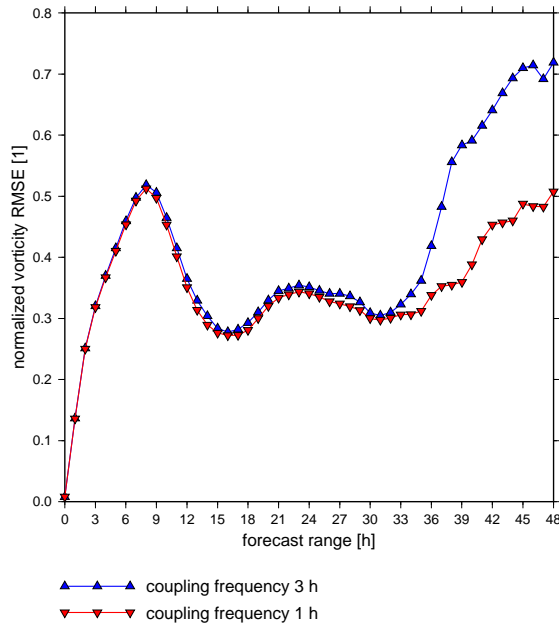


Figure 11: Sensitivity to coupling frequency for filtered LBC. Evolution of normalized vorticity RMSE at 500 hPa level computed over nested domain DOM1 without 8 point boundary zone. Nested runs with perfect initial state and coupling frequencies 3 h and 1 h.

to be superior to 3 hour coupling frequency after roughly 33 hours, which is significantly later than in perfect twin experiment. This is not so surprising when one realizes that filtering of LBC removed short scales which are often associated with high frequencies.

Removal of high frequencies makes LBC evolution smoother and mitigates problem of their undersampling.

It should be remembered, however, that all conclusions concerning coupling frequency were obtained for single case and should be generalized with caution. For example, positive impact of 1 hour coupling frequency with respect to 3 hour coupling frequency becomes much more pronounced in situations where small, rapidly moving weather system enters LAM domain.<sup>6</sup>

### 3.4 Comparison of linear and quadratic couplings

So far all experiments were done with LBC quadratically interpolated in time. It is interesting to ask what would be the impact if these interpolations were linear. In order to see this, perfect twin experiment and experiment with perfect initial state and filtered LBC were repeated, both with 3 hour coupling frequency and LBC interpolations linear in time (LQCPL = .F.).

Results are presented on figure 12. It can be said that impact of linear coupling is neutral regardless if perfect LBC (plot 12a) or filtered LBC (plot 12b) are used. There is no systematic deterioration of scores visible. This implies that for 3 hour coupling frequency use of linear coupling should be fully sufficient. However, going to finer horizontal resolutions might invalidate this result since it will increase proportion of high frequency phenomena resolved by driving model. When horizontal resolution is kept constant, increase of coupling frequency should further diminish difference between linear and quadratic couplings.

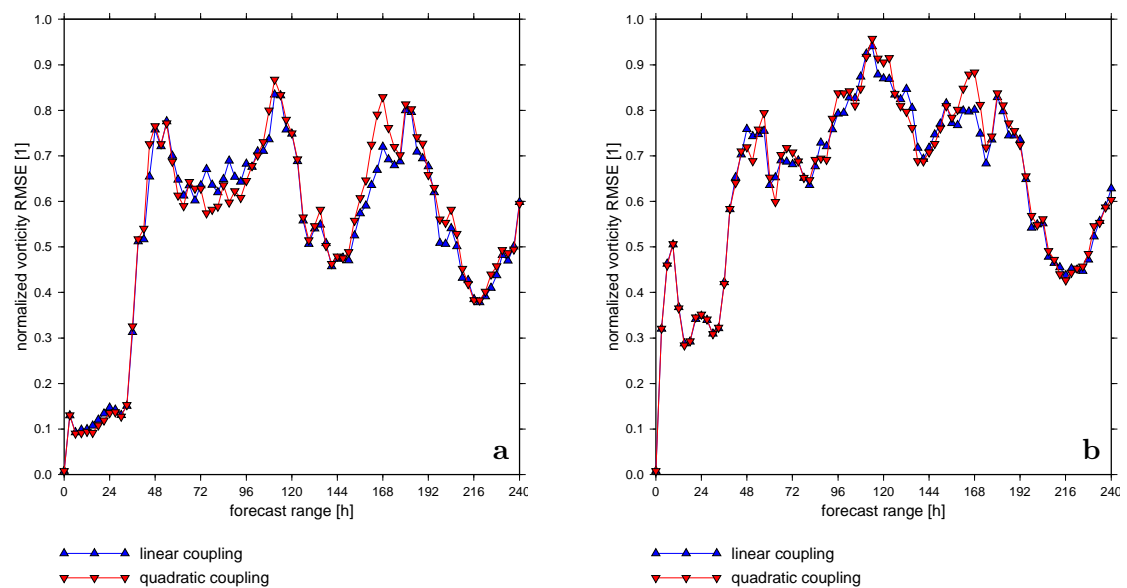


Figure 12: Comparison of linear and quadratic couplings. Evolution of normalized vorticity RMSE at 500 hPa level computed over nested domain DOM1 without 8 point boundary zone. Nested runs with perfect initial state used perfect (a) and smoothed (b) LBC.

<sup>6</sup>According to Claude Fisher such system is typically called X-mas storm.

### 3.5 Impact of biperiodicization and “problem” of ultralong waves

In order to estimate impact of biperiodicization, twin experiment with 1 hour coupling frequency was repeated with extension zone enlarged from 11 to 21 points. It means that size of C + I + E zone was  $160 \times 160$  points with spectral truncation  $79 \times 79$  (linear grid). Wider extension zone means smoother biperiodicization of fields with less Gibbs waves generated inside physical domain. Therefore, derivatives computed in spectral space should be more accurate.

Scores obtained with 11 and 21 point extension zone were almost identical (not shown). It means that default 11 point extension zone is fully sufficient for reliable biperiodicization of fields.

For spectral LAM question about representation of ultralong waves (i.e. waves longer than size of domain) is often raised. Common worry is that such waves might not propagate correctly because after biperiodicization they will be projected to shorter waves which may have different phase velocities (this is the case both for Rossby and gravity modes). Superficial analysis then suggests that monochromatic ultralong wave from driving model will not only propagate with wrong velocity in nested spectral LAM, but it will also be gradually distorted.<sup>7</sup>

Fortunately for spectral LAM given reasoning is misleading as it ignores role of lateral coupling. It would be true if the spectral LAM was integrated without any coupling. Such solution would not respect LBC, which makes it unphysical. It would allow propagation of artificial signal from extension zone to physical C + I domain. As soon as coupling scheme is active it modifies spectral coefficients in every timestep. This forcing, although localized in physical space, is non-local in space of spectral coefficients. That is why analysis of “free” modes which ignored this additional source of forcing was wrong. In other words, one must be very careful when generalizing results of Fourier analysis to non-periodic domain.

The only complications specific for spectral LAM are biperiodicization and spectral fitting of fields. They should be done in such way which generates minimum of Gibbs waves in physical C + I domain. When spectrally computed derivatives in nested LAM are close to derivatives computed in driving model (spectral or not), there should be no worry about ultralong waves. This conclusion is in full agreement with results of Boyd [1].

### 3.6 Spectral composition of RMSE

Finally, spectral composition of vorticity RMSE for nested run with perfect initial state and filtered LBC will be examined. It enables to estimate how much forecast skill comes from short scales which are of primary interest for LAM. Lack of skill in these scales would put usefulness of LAM approach in question.

Figure 13 shows spectral profiles of vorticity RMSE and its relative value with respect to imperfect driving solution for 5 different pressure levels. As in figure 3, horizontal axis contains relative cut-off wavenumber  $r = k/k_{\max}$ . All wavenumbers greater than  $r k_{\max}$  were filtered out from forecasted vorticity field before computing the scores. This time scores were averaged over days 3–10 (with step 12 hours), in order to exclude period of initial error growth.

Plot 13a shows that unfiltered vorticity field ( $r = 1$ ) has highest RMSE at 500 hPa level and lowest RMSE at 925 hPa level. From spectral composition it can be seen that

---

<sup>7</sup>Careful reader have spotted already that if this reasoning was correct it would apply not only to ultralong waves, but to every wave  $\exp[i(k_x x + k_y y)]$  for which size of nested C + I + E domain  $L_{x,y}$  is not integer multiple of  $2\pi/k_{x,y}$ .

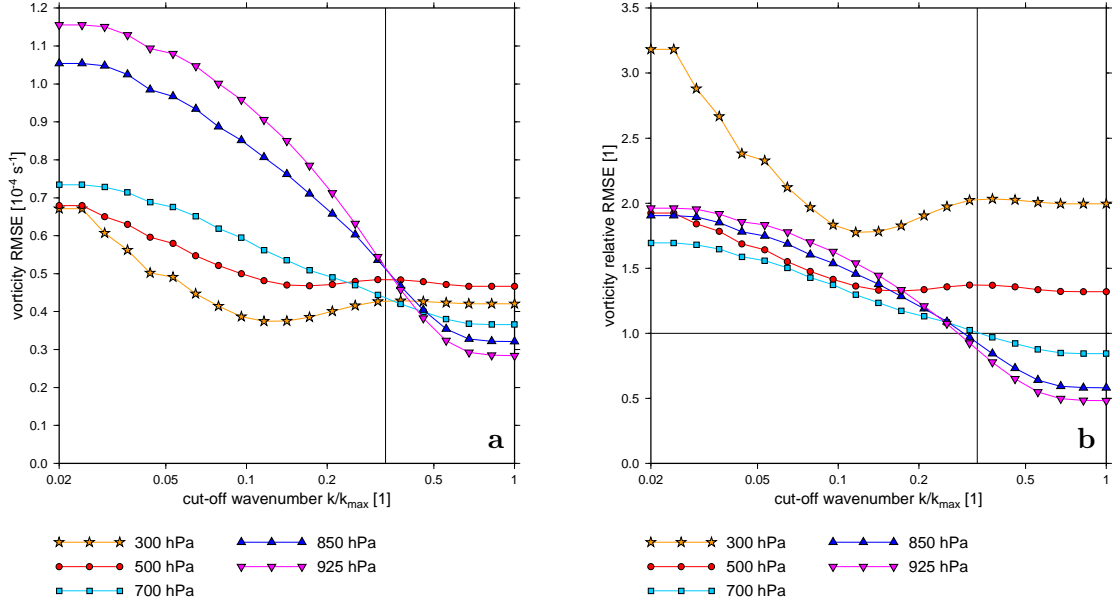


Figure 13: Dependency of vorticity RMSE (a) and its relative value with respect to imperfect driving solution (b) on relative cut-off wavenumber. Nested run with perfect initial state and filtered LBC. Errors computed over nested domain DOM1 without 8 point boundary zone and averaged over integration days 3–10. Vertical line denotes value  $r_2^{\text{crit}}$  which was used for LBC filtering. Horizontal line  $y = 1$  on plot (b) shows usability limit for nested run. Above this line quality of nested solution is worse than quality of driving solution.

while for 925 and 850 hPa levels addition of intermediate scales significantly reduces forecast error, at 700 hPa level their positive impact is less pronounced but dependency is still monotonic. Qualitative behaviour changes for 500 and 300 hPa levels where error reaches minimum somewhere between  $r = 0.1$  ( $\lambda = 20\Delta x$ ) and  $r = 0.2$  ( $\lambda = 10\Delta x$ ). For these levels addition of shorter scales does not bring any benefit, it can even deteriorate scores.

Cardinal question of LAM approach is how much improvement brings high resolution nested solution with respect to low resolution driving solution. Added value of nested forecast can be measured by comparing its RMSE scores against RMSE scores of fields diagnosed from filtered LBC which represent imperfect driving model.

Plot 13b reveals that nested forecast brings largest improvement for levels 925 and 850 hPa where vorticity RMSE is reduced to roughly one half of the value obtained from filtered LBC. Slight RMSE reduction is still visible at 700 hPa level. For all these levels improvement comes mostly from wavelengths which were filtered out from LBC. Situation is different for levels 500 and 300 hPa where nested model spoils vorticity field and there is no skill in short scales. Even if these scales are removed from nested solution, RMSE remains larger than for filtered LBC.

Added value of nested LAM forecast close to the ground can be attributed mainly to improved representation of surface and strong interaction between surface and atmospheric boundary layer. Important fact is that positive impact remains visible even for long forecast lead times. On the other hand, deterioration of scores at higher levels which reaches full strength within initial 48 hours constitutes serious limitation for usability of LAM approach.

---

In this section basic properties of Davies relaxation scheme were analyzed using perfect model approach. It was seen that for given domain size and resolution impact of initial state becomes very weak after 48 hours. On the other hand, accurate initial state significantly improved forecast during early hours of integration. Test with zero relaxation zone enabled to evaluate improvement due to Davies relaxation scheme itself. LBC interpolations linear in time were sufficient already for 3 hour coupling frequency. Providing LBC more often than every hour hardly had any impact. Biperiodicization procedure used in ALADIN works satisfactorily with 11 point extension zone and there is no problem with ultralong waves. After period of initial error growth nested model still improves forecast of imperfect driving model at lower levels, but deteriorates it at higher levels where short scales lost their predictive skill.

## 4 Conclusions

Diagnostic tool based on perfect model approach [3] was developed and some basic tests of Davies relaxation scheme in 3D hydrostatic ALADIN were performed. Based on the results, some recommendations for carrying out coupling experiments can be formulated:

- For geographical domain approximately  $1300 \times 1300$  km error caused by coupling scheme reaches saturation within 48 hours. It means that for this domain size 2-day integration is sufficient to see full impact of coupling. It can be expected that for smaller domains this time will be even shorter.
- Statistically significant results can be obtained by one long term integration of nested model with scores being averaged over integration window without initial period of error growth. Better coupling scheme should have smaller asymptotic error. When the initial error growth is of interest, scores from several shorter integrations should be averaged.
- In order to reduce spinup problem, experiments with perfect initial conditions and filtered lateral boundary conditions can be carried out.
- Suitable field to be monitored is vorticity at 500 hPa level. It is not so strongly affected by orography as vorticity at lower levels and it contains smaller proportion of shortest waves. Despite having smaller variability this level is most sensitive to lateral boundary treatment.
- Visual inspection of vorticity field and its error is instructive, but some objective scores are needed for more sensitive comparison. First of all, nested run should correctly reproduce variance of perfect model reference. Distance from reference solution can be measured by RMSE normalized by standard deviation of reference solution. As pointed out by Elía et al. [3], RMSE is rather strict criterion since it heavily penalizes phase errors of small scales even if their amplitudes are forecasted well. And for small scale systems even slight shift in time can cause significant phase errors. From this point of view RMSE can be unnecessarily strong criterion for evaluating quality of nested integration. Anyway, point interpretation of high resolution LAM forecasts requires sufficiently good RMSE scores.
- Valuable information can be obtained by analysing spectral composition of scores. Perfect total variance does not mean much when its spectral composition differs significantly from reference.

- When perfect LBC are used, increase of coupling frequency from 3 h to 1 h brings significant error reduction after spinup period. Further increase of coupling frequency does not bring any additional improvement. For filtered LBC positive impact of 1 h coupling frequency appears later and is not so strong. This is not surprising because LBC filtering removed shortest scales which are often associated with high frequencies undersampled by coupling scheme. Coupling frequencies higher than 1 h can become useful for finer horizontal resolutions.
- For 3 h coupling frequency linear and quadratic couplings perform about equally on average, regardless of whether perfect or filtered LBC are used. In some periods quadratic coupling outperforms linear one and vice versa. In such circumstances use of linear coupling should be fully sufficient. It can be expected that for higher coupling frequencies difference between linear and quadratic couplings will further diminish.

Recommendations denoted by circle (○) may depend on domain size, geographical location, horizontal resolution and relative cut-off wavenumber used for filtering LBC. They should be revisited if these are changed significantly. Recommendations denoted by bullet (●) should have more general validity.

Diagnostic tool is now ready to evaluate any alternatives or improvements of current ALADIN coupling scheme. When using it, one should be aware that perfect model approach is idealized and has its limitations. It gives valuable estimate of errors coming from coupling scheme itself, but it says nothing about total error when LBC provided by driving model are not just filtered true state. It also cannot address errors caused by use of nested model different from driving model. In such situation nested model often requires fields which are not available in driving model (e.g. non-hydrostatic fields or water species). In this case perfect model approach can at least be used to analyze spinup coming from invented values of missing fields in initial state and LBC.

## Appendix

### A Where to find what

Integration scripts, output listings, input and output FA files can be found on `sx68`. Some of directories are symbolic links, with data being physically located under `/work/` directory:

|                                |   |
|--------------------------------|---|
| <code>~mma157/coupling/</code> | root directory  |
| <code>  clim/</code>           | climate files (only used for EE927 <code>arp</code> → <code>mfstep</code> ) |
| <code>  fpos/</code>           | postprocessing files (selected fields on 5 pressure levels)                 |
| <code>    dom1j1/</code>       | experiments on domain DOM1, unfiltered LBC                                  |
| <code>    dom1j3/</code>       | experiments on domain DOM1, filtered LBC                                    |
| <code>    mfstep/</code>       | reference experiment on domain MFST   |
| <code>  icmsh/</code>          | historical files  |
| <code>    dom1j1/</code>       | experiments on domain DOM1, unfiltered LBC                                  |
| <code>    dom1j3/</code>       | experiments on domain DOM1, filtered LBC                                    |
| <code>    mfstep/</code>       | reference experiment on domain MFST   |
| <code>  lbc/</code>            | coupling files  |
| <code>    arp/</code>          | low resolution LBC from ARPEGE  |
| <code>    dom1j1/</code>       | LBC for domain DOM1, unfiltered   |
| <code>    dom1j3/</code>       | LBC for domain DOM1, filtered   |
| <code>    mfstep/</code>       | LBC for domain MFST   |
| <code>  script/</code>         | integration scripts and output listings                                     |
| <code>  README</code>          | description of experiments  |

In order to release disk space, some FA files had to be moved to `archiv` where they are kept in the same directory tree under user `mma157`.

All scripts were written in perl. In order to use them, one must add path

```
/home/mma/mma157/lib/perl
```

into enviromental variable `PERLLIB`. It tells perl where to look for local modules. NQS jobs based on perl scripts must be submitted using command `qsub -x`, so that user environment is copied for the job.

Used masters are stored on `archiv`:

|  |                   |
|--|-------------------|
| <code>~mma157/bin/</code>                      |                   |
| <code>  master_al29t2mx1_mfstep_01_sx68</code> | modification 1    |
| <code>  master_al29t2mx1_mfstep_03_sx68</code> | modification 1, 2 |

They are based on cycle `al29t2mx1` with two minor modifications:

1. Maximum truncation `JPXTRO` increased to 300 (`xrd/fa/facomp.h`). This was needed for reference experiment on domain MFST where zonal truncation was 299.
2. Namelist values `NBZONL`, `NBZONG` not overwritten by values read from input FA file (`ald/setup/suedim.F90`). This enabled to run experiments with different widths of relaxation zone using the same coupling files.

Developed FA utilities for LBC filtering and computation of scores are stored in CVS on `voodoo` under project `fautils_coupling`. They should be compiled on `kappa` and

run on `sx68` where the executables can be found:

---

```
~mma157/opt/bin/  
fa_filter  
fa_sp2gp  
fa_stat
```

---

## B Brief description of developed FA utilities

Three utilities for manipulating FA files with ALADIN geometry were created:

---

**fa\_filter** – applies cosine spectral filter on selected fields in FA file

---

Fields to be filtered can be both gridpoint and spectral. When gridpoint field is to be filtered and input FA file does not contain extension zone, size of C + I + E zone which will be used for biperiodicization must be supplied by user. Biperiodicization procedure is the same as in model ALADIN. Spectral filter can be tuned by setting critical relative wavenumbers  $r_1^{\text{crit}}$  (end of pass band where filtering function is identically 1) and  $r_2^{\text{crit}}$  (start of stop band where filtering function is identically 0).

---

**fa\_sp2gp** – converts all spectral fields found in FA file to gridpoint fields

---

This is handy when one wants to visualize spectral fields without running fullpos. It creates output FA file which contains same fields as input FA file, but they are all in gridpoint representation. Packing of fields is preserved.

---

**fa\_stat** – compares selected field in 2 FA files and computes basic statistics

---

Returned scores are bias ( $\text{file2} - \text{file1}$ ), RMSE difference ( $\text{file2} - \text{file1}$ ) and standard deviations ( $\text{file1}$ ,  $\text{file2}$ ). They are computed over C + I domain, but user defined boundary zone can be omitted.

When run without arguments, utilities display command line help. For namelist driven utilities it contains also example of namelist file and explanation of all namelist variables. More detailed info can be found in corresponding source codes under CVS.

## C Important remark on vorticity postprocessing

When using fullpos, one should be aware that *definition* of postprocessed vorticity field depends on namelist settings. It would be natural to expect that postprocessing on pressure levels gives vorticity defined by formula (2). However, this is true only if dynamical fields are spectrally fitted after vertical interpolations. In such case vertically interpolated quantities are wind components. Their horizontal derivatives are computed only afterwards, i.e. along pressure levels. Order of operations changes when spectral fitting is turned off – vorticity is diagnosed on eta levels and then interpolated to pressure levels. In this case horizontal derivatives of wind components are computed along eta levels, what means that output vorticity field will be significantly different from field (2) above steep orography.<sup>8</sup>

Following table summarizes namelist settings which influence definition of vorticity postprocessed on *pressure* levels:

---

<sup>8</sup>This difference will diminish with height thanks to flattening of eta levels.

|   | NAMFPC  |       | NAMAFN       | output representation | hor. derivatives computed along |
|---|---------|-------|--------------|-----------------------|---------------------------------|
|   | CFPFMT  | LFITP | TFP_VOR%LLGP |                       |                                 |
| 1 | 'LELAM' | .T.   |              | gridpoint             | pressure levels                 |
| 2 | 'LELAM' | .F.   |              | gridpoint             | eta levels                      |
| 3 | 'MODEL' |       | .T.          | gridpoint             | eta levels                      |
| 4 | 'MODEL' |       | .F.          | spectral              | pressure levels                 |

It is clear from the table that vorticity defined by formula (2) is obtained only for configuration 1. In principle it could be obtained also with configuration 4, but in such case output field would have to be converted to gridpoint space by external utility. Forcing gridpoint representation by setting `TFP_VOR%LLGP = .T.` (configuration 3) would be a serious mistake since it changes order of vertical interpolations and computation of horizontal derivatives.

## References

- [1] Boyd, J. P., 2005: Limited-area Fourier spectral models and data analysis schemes: windows, Fourier extension, Davies relaxation, and all that. *Mon. Wea. Rev.*, **133**, 2030–2042.
- [2] Durran, D. R., 2001: Opened boundary conditions: fact and fiction. *IUTAM Symposium on Advances in Mathematical Modelling of Atmosphere and Ocean Dynamics*, P. F. Hodnett, Ed., Kluwer Academic Publishers, pp. 1–18.
- [3] Elía, R., R. Laprise, and B. Denis, 2002: Forecasting skill limits of nested, limited-area models: a perfect-model approach. *Mon. Wea. Rev.*, **130**, 2006–2023.